Acta Neuropathologica (2024) 148:55
https://doi.org/10.1007/s00401-024-02815-w

ORIGINAL PAPER

Hypothesis-based investigation of known AD risk variants reveals the genetic underpinnings of neuropathological lesions observed in Alzheimer's-type dementia

Celeste Laureyssen[1,2] · Fahri Küçükali[1,2] · Jasper Van Dongen[1,2] · Klara Gawor[3] · Sandra O. Tomé[3] · Alicja Ronisz[3] · Markus Otto[4] · Christine A. F. von Arnim[5] · Philip Van Damme[6,7] · Rik Vandenberghe[7,8] · Dietmar Rudolf Thal[3,9] · Kristel Sleegers[1,2]

Received: 16 July 2024 / Revised: 8 October 2024 / Accepted: 8 October 2024

Abstract

Alzheimer's disease (AD) is the leading cause of dementia worldwide. Besides neurofibrillary tangles and amyloid beta (Aβ) plaques, a wide range of co-morbid neuropathological features can be observed in AD brains. Since AD has a very strong genetic background and displays a wide phenotypic heterogeneity, this study aims at investigating the genetic underpinnings of co-morbid and hallmark neuropathological lesions. This was realized by obtaining the genotypes for 75 AD risk variants from low-coverage whole-genome sequencing data for 325 individuals from the Leuven Brain Collection. Association testing with deeply characterized neuropathological lesions revealed a strong and likely direct effect of rs117618017, a SNP in exon 1 of *APH1B*, with tau-related pathology. Second, a relation between *APOE* and granulovacuolar degeneration, a proxy for necroptosis, was also discovered in addition to replication of the well-known association of *APOE* with AD hallmark neuropathological lesions. Additionally, several nominal associations with AD risk genes were detected for pTDP pathology, α-synuclein lesions and pTau-related pathology. These findings were confirmed in a meta-analysis with three independent cohorts. For example, we replicated a prior association between *TPCN1* (rs6489896) and LATE-NC risk. Furthermore, we identified new putative LATE-NC-linked SNPs, including rs7068231, located upstream of *ANK3*. We found association between *BIN1* (rs6733839) and α-synuclein pathology, and replicated a prior association between *USP6NL* (rs7912495) and Lewy body pathology. Additionally, we also found that *UMAD1* (rs6943429) was nominally associated with Lewy body pathology. Overall, these results contribute to a broader general understanding of how AD risk variants discovered in large-scale clinical genome-wide association studies are involved in the pathological mechanisms of AD and indicate the importance of downstream elimination of phenotypic heterogeneity introduced in these studies.

Keywords Alzheimer's disease · *APH1B* · *APOE* · *PTK2B* · *BIN1* · *USP6NL* · *UMAD1* · *ANK3* · *TPCN1* · *SLC2A4RG* · Neuropathology · Genetics

✉ Kristel Sleegers
kristel.sleegers@uantwerpen.be

1 Complex Genetics of Alzheimer's Disease Group, VIB-UAntwerp Center for Molecular Neurology, University of Antwerp, Campus Drie Eiken, Universiteitsplein 1, 2610 Antwerp, Belgium

2 Department of Biomedical Sciences, University of Antwerp, Antwerp, Belgium

3 Laboratory for Neuropathology, Department of Imaging and Pathology, and Leuven Brain Institute, KU Leuven, Louvain, Belgium

4 Department of Neurology, Martin-Luther-University Halle-Wittenberg, Halle (Saale), Germany

5 Department of Geriatrics, University Medical Center Göttingen, Göttingen, Germany

6 Laboratory for Neurobiology, VIB-KU Leuven, Louvain, Belgium

7 Department of Neurology, UZ Leuven, Louvain, Belgium

8 Laboratory for Cognitive Neurology, Department of Neurosciences, KU Leuven, Leuven Brain Institute, Louvain, Belgium

9 Department of Pathology, University Hospital Leuven, Louvain, Belgium

Published online: 18 October 2024

Introduction

In the broad spectrum of modern-day diseases, few are so complex and elude a complete understanding as Alzheimer's disease (AD). This insidious form of dementia imposes a grave burden upon the daily lives of patients and family. The first disease-modifying treatments are now emerging [59, 63]. However, they only focus on one aspect of the pathological profile of AD and have limited efficacy in slowing cognitive decline. This indicates that the pathogenesis underlying the disease remains to be unraveled further. Besides the development of novel treatments, the extensive preclinical phase of AD offers significant opportunity for early detection and intervention [56]. Therefore, the strong genetic background of AD, with an estimated heritability of 60–80% [7], offers added value for genetic studies to identify early therapeutic targets and risk genes underlying disease mechanisms to elucidate the biological pathways involved in the development of the disease and aid in the discovery of biomarkers.

A definite diagnosis of AD can only be made after a post-mortem examination in which the presence of the neuropathological hallmarks of AD is confirmed. These hallmarks comprise extracellular plaques of aggregated $A\beta_{1\text{-}42}$ protein and intracellular, neurofibrillary tangles composed of hyperphosphorylated tau protein (pTau) [33]. These hallmark lesions are accompanied by a general state of neuroinflammation, ultimately resulting in neuronal loss. Tangles and plaques are rarely the sole neuropathological phenotypes observed in the AD brain. Additional co-morbid lesions are present in the majority of cases which could have a synergistic effect on the clinical presentation and disease progression.

Cerebral amyloid angiopathy (CAA) is a frequently observed co-morbidity in AD and is characterized by the accumulation of Aβ in blood vessel walls, occurring in over 90% of AD cases [32]. There are two types of CAA, Type I and Type II. CAA type I distinguishes itself from type II by the presence of Aβ deposits in the cortical capillaries, additional to Aβ inclusions in the leptomeningeal and cortical vessels [61]. Genetically, a distinction can be made since the frequency of *APOE* ε4 alleles is up to four times higher in CAA type I cases compared to type II and controls. CAA in the brain of AD cases can contribute to the clinical gravity of the disease by increasing risk for weakening of the vessel wall, eventually resulting in ruptures. Granulovacuolar degeneration (GVD) bodies are membrane-bound vacuolar structures containing dense protein granules. GVD bodies are most frequently observed in hippocampal pyramidal neurons of patients with AD and other tauopathies. It was hypothesized that GVD can be induced by tau accumulation [66] and the two pathologies often co-occur in the brain. Evidence has also shown a direct relation between GVD and a cell-death mechanism referred to as necroptosis, posing that GVD is in fact a proxy for necroptosis [38]. Furthermore, GVD is associated with limbic-predominant age-related TDP-43 encephalopathy neuropathological changes (LATE-NC), with LATE-NC being suspected to aggravate GVD pathology [37]. LATE-NC is a pathology where phosphorylated transactive-response DNA binding protein 43 (pTDP-43) accumulates in the neuronal cytoplasm. TDP-43 inclusions in the brain are hallmark lesions of frontotemporal lobe degeneration with TDP-43 brain pathology (FTLD-TDP) and amyotrophic lateral sclerosis (ALS). However, inclusions are also observed in up to 70% of symptomatic AD cases [43]. Genetically, LATE-NC has been associated with 5 risk genes: *TMEM106B*, *GRN*, *KCNMB2*, *ABCC9* and *APOE* [48]. TDP-43 inclusions have been associated with a more severe clinical profile of AD [34], indicating that it is an important co-morbidity in AD pathology. Another pathology coinciding with AD is the presence of α-synuclein inclusions observed as Lewy bodies and Lewy neurites [57]. Lewy body dementia (LBD) accounts for an average 5% of reported dementia cases [35] and can occur alongside AD, resulting in a form of mixed dementia. Reports show that up to 50% of AD cases have co-morbid Lewy bodies in the neocortical and limbic brain regions [23]. Several genes have been linked to Lewy body dementia with some overlap with the genetic risk profile of AD and PD as well as some unrelated genes. Some examples are *APOE*, *SNCA*, *GBA* and *LRRK2* [50].

Genome-wide association studies (GWAS) are rapidly discovering common (MAF > 0.01) genetic variation associated with disease. Some examples of the earliest associated loci are *BIN1*, *CLU*, *CR1* and *PICALM* [26, 40, 71]. Now, over 75 genetic loci have been associated with sporadic AD [5]. Pathway enrichment analysis of genes located in or prioritized to these loci has highlighted a variety of biological pathways, pointing to intuitive disease mechanisms, like APP and tau processing, as well as pathways like endocytosis, lipid metabolism and innate immunity [31, 39, 65, 69]. GWASs for AD have mainly been using clinical AD diagnosis as the predicted variable in regression models due to the necessity of ever-increasing sample sizes to gain sufficient statistical power for detecting more significant relations. Another valuable approach would be to use specific endophenotypes observed in AD pathogenesis. Endophenotypes have proven to add value for risk variant discovery using them as predicting variables in regression models in GWASs. Investigating association with endophenotypes, like CSF or serum biomarker levels and brain imaging has allowed the discovery of novel risk loci and confirmation of various loci discovered with case–control designed studies [27, 30, 41]. In this study, a hypothesis-based investigation

of several known AD risk genes and their contribution to individual neuropathological lesions was performed in a European cohort of 325 individuals aged 50 or older at death. Our analyses highlight the importance of *APOE* in AD pathogenesis and uncover additional strong associations between a known AD risk variant situated in *APH1B* and several distinct neuropathological phenotypes.

Methods

Cohort

The analyses were performed on the Leuven Brain Collection, which includes human brain tissue received from university or municipal hospitals in Leuven (Belgium), Bonn, Offenbach am Main and Ulm (Germany). Collection was in accordance with the local ethical committee guidelines and laws regarding the use of human tissue for research. Brains of 325 individuals were included in the present study, aged 50 years or older at death. Individuals were labeled as AD when they were clinically diagnosed with dementia (based on the CDR score) and had at least an intermediate degree of AD neuropathological change (ADNC) according to NIA-AA criteria (ABC score) [28]. Individuals without dementia but with ADNC were labeled as asymptomatic AD. Individuals with no ADNC were labeled as 'noAD', meaning they had no AD pathology, but not excluding the presence of other pathologies, thus comprising individuals with healthy brains as well as individuals suffering from neurodegenerative brain diseases without ADNC. For each individual, 500 mg fresh frozen cerebellar tissue was stored in Biobank Antwerp, Antwerp, Belgium; ID: BE 71030031000 for DNA extraction.

Staging and staining of neuropathological lesions

Staging and staining of the lesions was performed at the Laboratory of Neuropathology at the KU Leuven. Neurofibrillary tangles were stained using an AT8 phospho-tau monoclonal antibody (Thermo Fisher Scientific, United States) in a 1:1000 dilution and/or with the Gallyas silver staining method. Braak stage was determined as described elsewhere, with stages I and II indicating the presence of tangles in the entorhinal cortex, stage III and IV the spread to hippocampus and the limbic system, stage V spread to the neocortex and finally the most advanced stage VI where tangles are numerously present throughout the neocortex [10]. CERAD score was also assessed on a staining with an AT8 antibody, scored 0-III ranging from no neuritic plaque pathology to severe and widespread neuritic plaques [44]. The use of the AT8 phospho-tau immunohistochemistry for detecting neuritic plaques has been chosen since immunohistochemical stainings are more reproducible than silver methods such as the Bielschowsky staining [2] and the consensus guidelines allow Gallyas or anti-tau immunohistochemistry for neuritic plaque detection [29]. Aβ staining was performed using an 4G8 antibody against A$\beta_{17\text{-}24}$ (Biolegend, USA) in a 1:5000 dilution. Aβ score in the medial–temporal lobe (MTL) reflects the spread of Aβ in the MTL in four phases [62]. The severity score of CAA was determined according to Vonsattel et al. [64]. TDP43 lesions were stained using a rabbit antibody against pTDP-43 S409/10 (Cosmobio Co., Japan) in a 1:5000 dilution after heat pretreatment at pH 6. pTDP staining was used to determine LATE-NC stages as well as GVD stages. LATE-NC was staged according to consensus guidelines [48] with three distinct stages: in stage I, TDP lesions are restricted to the amygdala or are present only in the hippocampus, stage II indicates lesions in both amygdala and hippocampus and in stage III the middle frontal gyrus is involved. GVD stages were determined based on earlier described guidelines [49]. In stage I, GVD lesions are restricted to the CA1/2-subiculum region, in stage II, the entorhinal cortex and/or CA3-4 are affected together with the basal nucleus of Meynert. Stage III indicates additional involvement of the temporal neocortex and in stage IV, the amygdala and/or hypothalamus are affected as well. In stage V, the pathology is widespread and affects the oral raphe nuclei, pedunculopontine tegmental nucleus, cingulate gyrus, thalamus, and the frontal and parietal neocortex. Inclusions of α-synuclein were stained using an anti-α-synuclein antibody, clone 5G4 (Merck Life Science, Belgium) in a 1:2000 dilution. Staging was performed following the Braak scoring system for Parkinson's disease (PD) [11]. Stage I describes Lewy bodies restricted to the olfactory bulb and dorsal motor nucleus of the vagal nerve. In stage II, the brainstem and locus coeruleus become involved, whereas in stage III, there is a spread of the pathology to the substantia nigra and other brainstem regions. Stage IV indicates spread of Lewy body pathology to the limbic system, affecting the hippocampus and the amygdala. In stage V, the neocortex is affected and in the most advanced stage, stage VI, the pathology is widespread throughout the neocortex. Finally, general AD pathology was described by the NIA-AA classification system (ABC score), which is a score compiled by Braak NFT score, Aβ score and CERAD score, indicating the level of AD pathology (absent, low, intermediate or high) [28].

DNA extraction and quality control

DNA was extracted from fresh frozen cerebellar tissue using a QIAGEN DNeasy 96 Blood & Tissue kit (QIAGEN, Benelux). After extraction, an AMPure XP magnetic bead (Beckman Coulter life sciences, Analis, Belgium) purification was done to remove leftover waste products from the DNA

extraction process. Concentration of the extracted DNA was measured by UV/Vis (Trinean NV, Belgium) and normalized to 100 ng/µl based on initial dsDNA concentrations. Normalized plates were subjected to an additional concentration measurement using a Qubit Quant-it kit (Thermo Fisher Scientific, Belgium) for validation. Quality of the extracted DNA was investigated using an Agilent Fragment Analyzer Capillary array (Agilent Technologies, Belgium). The DNA was checked for fragment length and contamination peaks. In case of insufficient quality (concentration < 1 ng/µl), DNA extraction was repeated. *APOE* genotyping was performed on all individuals and for participants with pre-existing information on *APOE* genotype, cross-validation was performed.

AVITI low-coverage whole-genome sequencing

Genotype information was acquired using a low-coverage whole-genome sequencing approach. Library preparation was performed using the xGen cfDNA & FFPE DNA Library Preparation Kit (IDT, Belgium) with complementary xGen UDI 10nt primers (IDT, Belgium) for adding a specific barcode to each of the samples. The xGen cfDNA & FFPE kit utilizes a double adaptor ligation step, minimizing chimera or dimer formation, and is tailored for low-input materials. Afterward, library concentration was measured, and samples were pooled equimolarly. Sequencing was performed at the VIB Nucleomics Core (Ghent, Belgium) on an AVITI instrument (Element Bioscience, San Diego) which employs avidity chemistry for sequencing [3]. In short, this technique employs rolling circle amplification, creating DNA polonies. Subsequently, nucleotide identification is achieved by fixing multivalent nucleotide ligands on dye-labeled cores which form polymerase–polymer–nucleotide complexes, then binding the polonies. The resulting fluorescent signal can be detected, and base-calling can be performed from the raw fluorescent signals. AVITI sequencing has improved data quality and provides flexibility in the workflow, allowing the adjustment of the library pools in between sequencing runs. For our purpose, 325 samples were sequenced at an average depth of 1 × coverage, followed by imputation.

Data processing and imputation

Raw FASTQ files were aligned to GRCh38 genome build using the Burrows–Wheeler Alignment (BWA) tool. Alignment was followed by imputation using GLIMPSE (Genotype Likelihoods IMputation and PHasing mEthod) [53], a set of tools used for phasing and imputation of low-coverage whole-genome sequencing data. GLIMPSE utilizes a matrix of genotype likelihoods at all variable positions of the reference panel as input. Genotype likelihoods are then refined by iterative genotype imputation and haplotype phasing utilizing the Gibbs sampling procedure [53]. For this study, the 1000 Genomes haplotype reference panel [4] was employed. Data quality control was carried out with PLINK version 2.0, filtering out positions with a low imputation quality score ($R^2 < 0.3$) and rare variants (MAF < 0.01). Relatedness in the population was investigated, but no sample pairs exceeded a PI-HAT threshold of 0.125. From the 325 individuals, allele dosages were extracted for 85 AD risk variants [83 index variants described by Bellenguez et al. and two *APOE* SNPs, rs429358 and rs74121 (Supplementary Table 1)]). The imputation pipeline could not perform imputation on indels, excluding four variants (rs139643391, rs1160871, rs35048651 and rs149080927) from downstream analysis. Additionally, five variants did not pass the MAF threshold (rs143080277, rs72824905, rs141749679, rs75932628 and rs60755019) as expected based on earlier reported MAF. Finally, one variant in the *IGH* gene cluster locus was not imputed and thus also not included in further analysis (rs7157106).

Genotype validation with ONT multiplex assay

Imputation following low-coverage whole-genome sequencing (lcWGS) data results in genotype likelihoods rather than hard-called genotypes, entailing the use of allele dosages in downstream regression modeling. In order to assess the reliability of the genotypes assigned by GLIMPSE based on genotype likelihoods, an alternative genotyping strategy was applied to investigate the concordance for SNPs with significant associations. The selected SNPs were genotyped utilizing an in-house designed Oxford Nanopore Technology (ONT) multiplex assay. Primers for all SNPs were developed using primerBLAST. Primer pairs were pooled together in one plex. In short, a multiplex PCR (mPCR) was carried out per 96 samples with previously tested optimized conditions. PlatinumTaq polymerase was used as a DNA polymerase. After mPCR, a barcoding PCR (bPCR) was performed resulting in the attachment of a unique barcode to the amplified DNA fragments. Tapestation (Agilent Technologies) was utilized for assessment of sample length and concentration. Consecutively, samples were pooled equimolarly. Library preparation was performed using the ligation sequencing kit LSK110 (Oxford Nanopore Technology) according to the accompanying protocol. Sequencing was performed on a Flongle flow cell (Oxford Nanopore Technology). Sequencing reads were aligned to GRCh38 genome assembly and variant calling was performed using Longshot [18], generating a phased VCF file used for downstream QC and data analysis.

Statistical analysis

Data QC and association analyses were performed with PLINK 2.0 (version v2.00a2.3LM). For the 12 investigated phenotypes, either linear or logistic regression was applied to assess the relation between known AD risk variants and neuropathological lesions. Linear regression was applied for semi-quantitative phenotypes (i.e., stages of pathology or severity scores), whereas logistic regression was utilized for binary phenotypes (presence or absence of a certain lesion). Regression models were built, correcting for age and sex, using allele dosages as an independent variable. Bonferroni correction was applied for multiple testing with a significance cutoff of $p = 0.0006$, correcting for the number of SNPs that was independently investigated ($n = 75$). For the three SNPs where true significant associations were discovered, a concordance check was performed comparing the hard-called genotypes of the SNPs between the distinct sequencing approaches. To explore the relationship between neuropathological lesions and AD risk SNPs, construction of a graphical lasso model [21] and network visualization was accomplished using glasso and qgraph packages in R studio respectively. The model included significantly associated genotypes and phenotypes. Variables in the model were standardized followed by computation of the Spearman partial correlation matrix. Graphical lasso was then used to generate the sparse inverse covariance matrix applying an L1 penalty to promote sparsity. The regularization parameter (ρ) was chosen based on the Extended Bayesian Information Criterion (EBIC) [20] using the recommended EBIC hyperparameter ($\gamma = 0.5$). The robustness of the model was investigated by testing stability with the corStability function from the bootnet R package [19].

Meta-analysis

Validation of significant genotype–phenotype associations was realized by performing a meta-analysis of the discovery cohort summary statistics and published summary statistics [36] of the Religious Orders Study/Memory and Aging Project (ROSMAP) cohort [6], Alzheimer's Disease Sequencing Project (ADSP) and Alzheimer's Disease genetic Consortium (ADGC) [14, 47]. In these cohorts, association of AD risk variants was performed with dichotomized neuropathological phenotypes. Therefore, we harmonized the neuropathological phenotypes from the Leuven Brain Collection prior to meta-analysis. More specifically, for pTau pathology, Braak NFT stages 0–IV were set to '0' and Braak NFT stages V–VI were referred to as '1'. For the neuritic plaque score, CERAD scores 0–II were converted to '0' and a CERAD score of III was set to '1'. Neuropathological data regarding TDP43 pathology from LATE-NC stage, pTDP in CA1 and pTDP in dentate gyrus were combined into one score reflecting the total absence (0) or presence (1) in any of these variables of pTDP lesions. For α-synuclein, the discovery cohort phenotype reflecting the general presence (1) and absence (0) of α-synuclein pathology was used. Employing these four dichotomized variables, association testing was performed in PLINK 2.0 (version v2.00a2.3LM) correcting for age and gender. Resulting summary statistics were used for meta-analysis using METAL (version 2010-03-25) employing the standard scheme 'SAMPLESIZE', implementing the studies' respective sample sizes as weight for the meta-analysis. Respective sample sizes varied for each phenotype based on the availability of phenotypic data. Variants selected for meta-analysis had at least one association with $p < 0.05$ for a specific phenotype in the discovery association analysis.

Results

Table 1 presents the demographic and neuropathological characteristics of the samples of the Leuven Brain Collection included in this study. Of 325 individuals, 98 had ADNC and a clinical diagnosis of AD, 113 had ADNC without clinical AD, and 114 had no ADNC. This latter group included true controls but also patients with other neurodegenerative brain diseases, such as ALS, FTLD, PD, vascular dementia, and mixed neuropathological profiles. The samples were not systematically screened for known causal mutations in genes implicated in neurodegenerative brain diseases.

Hypothesis-based analysis on 75 AD risk variants

Regression models were generated for 12 neuropathological phenotypes, summarized in Table 1. The distinct phenotypes can be mapped to different parts of the AD neuropathological profile. These distinct parts being the hallmark pathological features of AD, such as the severity of AD pathology (ABC score), neuritic plaques (CERAD score), Aβ (Aβ score and CAA score) and pTau (Braak NFT stage and CERAD score) pathology, as well as co-morbid granulovacuolar degeneration (GVD stage), α-synuclein (Braak PD stage), TDP43 (presence in posterior middle temporal lobe, presence in dentate gyrus and LATE-NC stages).

Regression modeling was done for 75 AD risk variants which passed quality control. A complete overview of all (nominally) significant associations is depicted in Fig. 1. An overview of all SNPs that were investigated is provided in Table 2 and summary statistics are listed in Supplementary Table 1.

In total, 27 SNPs were at least nominally associated with one neuropathological phenotype ($p < 0.05$). Three of the SNPs, rs429358, rs7412 and rs117618017, retained significant associations with neuropathological

Table 1 Demographic and neuropathological characteristics of the study cohort of 325 individuals

	Total ($n=325$)	No AD ($n=114$)	Asymptomatic AD ($n=113$)	AD ($n=98$)
Demographics				
Age (Mean ± stdev)	71 ± 10	66 ± 10	72 ± 9	76 ± 9
Sex (% female)	58.7	51	66.3	58
APOE ε3/3 (%)	57.9	68.4	55.8	48
APOE ε3/4 (%)	24.9	12.3	29.2	34.7
APOE ε4/4 (%)	4.3	0	0.88	13.3
APOE ε2/3 (%)	11.7	17.5	12.4	4.1
APOE ε2/4 (%)	0.62	0	1.8	0
APOE ε2/2 (%)	0.62	1.8	0	0
Braak NFT stage				
Braak 0 (%)	8.3	20.2	2.7	1
Braak 1 (%)	36	48.3	42.5	14.3
Braak 2 (%)	25.2	22	33.6	19.4
Braak 3 (%)	13.5	8.8	17.7	14.3
Braak 4 (%)	6.2	0.9	2.7	16.3
Braak 5 (%)	5.5	0	0.9	17.4
Braak 6 (%)	5.2	0	0	17.4
Absent (%)	0	0	0	0
Aβ score				
A*β* score 0 (%)	38.5	100	8	2
A*β* score 1 (%)	15.1	0	31.9	13.3
A*β* score 2 (%)	14.2	0	30.1	12.2
A*β* score 3 (%)	12.6	0	17.7	21.4
A*β* score 4 (%)	19.4	0	12.4	50
Absent (%)	0.31	0	0	1
Granulovacuolar degeneration				
Stage 0 (%)	53.5	76.3	59.3	20.4
Stage 1 (%)	20	12.3	27.4	20.4
Stage 2 (%)	8.6	7	4.4	15.3
Stage 3 (%)	4.6	0	5.3	9.2
Stage 4 (%)	7.4	0.9	3.5	19.4
Stage 5 (%)	4	0	0	13.3
Absent (%)	1.9	3.5	0	2
TDP-LATE				
Stage 0 (%)	61.2	57.9	69.9	55.1
Stage 1 (%)	4.6	3.5	4.4	6.1
Stage 2 (%)	3.4	1.8	0.9	8.2
Stage 3 (%)	2.5	0	0.9	7.1
Absent (%)*	28.3	36.8	23.9	23.5
TDP presence				
TDP in CA1 (%)	14.5	11.4	8.9	24.5
Absent (%)	4	8.8	1.8	1
TDP in dentate gyrus (%)	10.8	10.5	5.3	17.4
Absent (%)	3.7	8.8	0.9	1
Braak α-*synuclein stage*				
Braak 0 (%)	74.5	80.7	77.9	63.3
Braak 1 (%)	7.4	8.8	7.1	6.1
Braak 2 (%)	1.5	0	1.8	3.1
Braak 3 (%)	2.5	3.5	1.8	2
Braak 4 (%)	5.2	2.6	4.4	9.2

Table 1 (continued)

	Total ($n=325$)	No AD ($n=114$)	Asymptomatic AD ($n=113$)	AD ($n=98$)
Braak 5 (%)	2.8	0	0.9	8.2
Braak 6 (%)	4.9	2.6	4.4	8.2
Absent (%)	1.2	1.8	1.8	0
α-synuclein presence				
α-synuclein positive (%)	24.6	17.5	20.4	37.8
Absent (%)	1.2	1.8	1.8	0
α-synuclein outside brainstem (%)	13.2	5.3	9.7	26.5
Absent (%)	1.2	1.8	1.8	0
CAA severity score				
CAA severity 0 (%)	59.4	93.9	55.8	23.5
CAA severity 1 (%)	15.1	3.5	23.9	18.4
CAA severity 2 (%)	22.8	1.8	18.6	52
CAA severity 3 (%)	2.8	0.9	1.8	6.1
Absent (%)	0	0	0	0
CERAD neuritic plaque score				
CERAD 0 (%)	74.5	100	84.1	33.7
CERAD 1 (%)	9.9	0	12.4	18.4
CERAD 2 (%)	8.9	0	1.8	27.6
CERAD 3 (%)	6.8	0	1.8	20.4
Absent (%)	0	0	0	0
ABC score				
ABC 0 (%)	35.1	100	0	0
ABC 1 (%)	42.5	0	87.6	39.8
ABC 2 (%)	12	0	11.5	26.5
ABC 3 (%)	10.5	0	0.9	33.7
Absent (%)	0	0	0	0

Percentages in each column show distribution of the lesions over the different stages for the respective phenotype and disease group (no AD, asymptomatic AD or AD). Absent shows the percentage of individuals for whom phenotype data are missing per neuropathological lesion

*TDP-LATE staging was not performed in cases with FTLD or ALS

markers after Bonferroni correction. rs429358 and rs7412 are both SNPs determining the *APOE* risk haplotype in exon four. Significant associations with rs429358 were found with six neuropathological phenotypes: Aβ score ($p=1.17\times10^{-12}$), CAA ($p=3.84\times10^{-10}$), Braak NFT stage $p=1.88\times10^{-07}$), CERAD score ($p=8.04\times10^{-08}$), ABC score ($p=1.12\times10^{-12}$) and GVD stage ($p=0.0003$). For rs7412, a significant association was found with ABC score ($p=1.30\times10^{-05}$) and with Aβ score ($p=7.22\times10^{-05}$). As expected, *APOE* SNPs contributed most to the variance of each trait they were associated with.

Rs117618017 is a $C>T$ polymorphism in exon 1 of *APH1B*, located on chromosome 15. The variant encodes a missense mutation on a protein level (p.T27I). We observed a significant association between rs117618017 and three neuropathological phenotypes: ABC score ($p=0.0001$), CERAD score ($p=0.0005$) and Braak NFT stage ($p=6.90\times10^{-07}$). Additionally, there was an indication for a relation between rs117618017 and Aβ score ($p=0.015$), CAA ($p=0.010$), LATE-NC stages ($p=0.034$) and GVD stage ($p=0.0007$), albeit not passing multiple testing correction. For all these observations, an increase in T allele dosage is associated with an increase in pathology levels.

Investigating top hit in APH1B on directly sequenced data

For the top hits, a concordance check comparing hard-called genotypes from lcWGS data with directly sequenced genotypes was performed. A concordance of 97.5% was reported for *APH1B* genotypes and for both *APOE* SNPs, a concordance of 99.7% was recorded (Table 3). For the top associated SNP, rs117618017, regression models were reconstructed with the associated phenotypes. However, for these models, hard-called genotypes acquired with the ONT approach were used to check whether these results are comparable to the results obtained with regression models constructed with allele dosages from imputed lcWGS data.

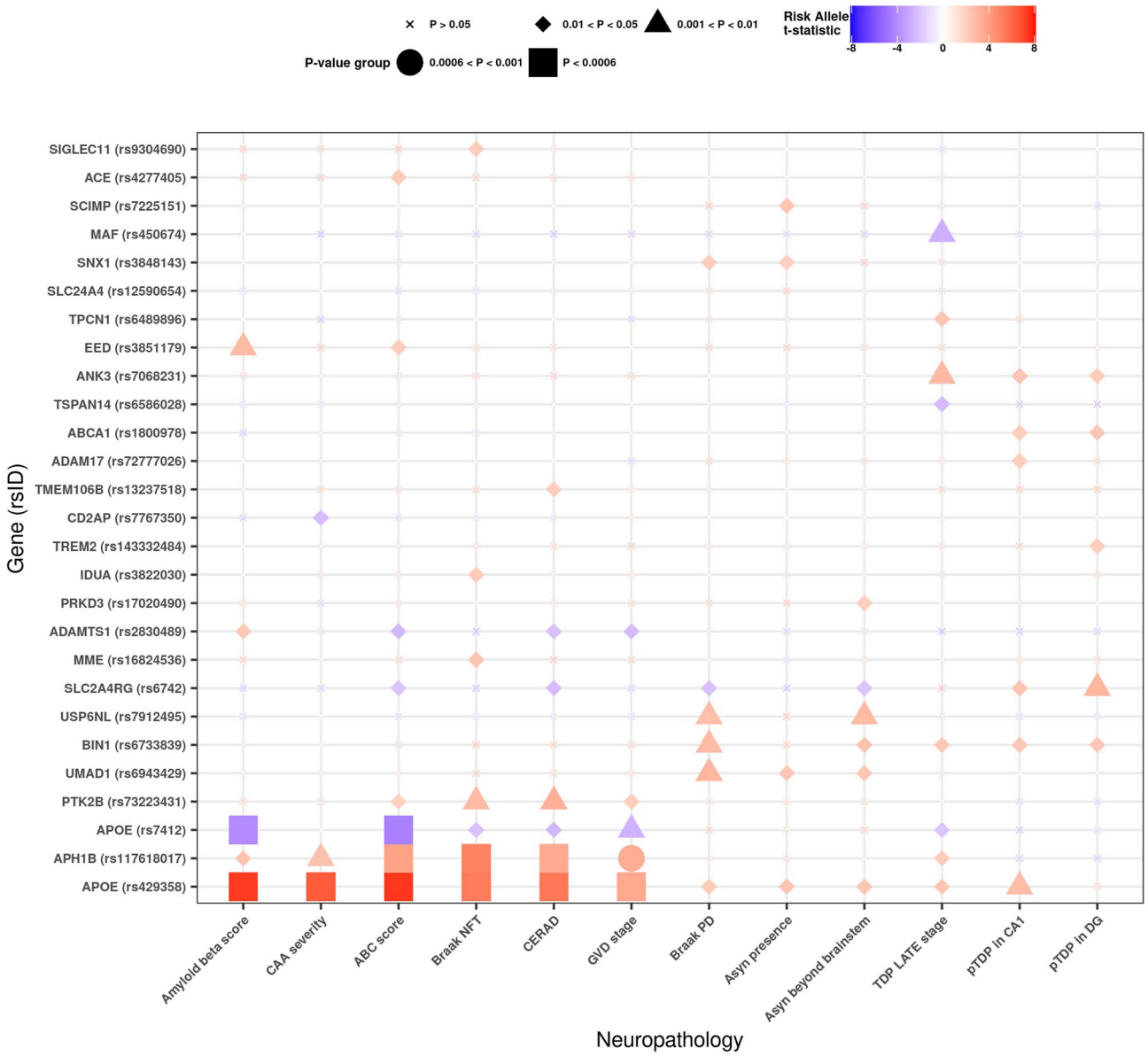

Fig. 1 Genotype–phenotype associations. 31 SNPs for which at least one nominal association with a neuropathological phenotype was discovered, are shown on the y-axis. The 12 investigated neuropathological phenotypes are listed on the x-axis. Each data point on the graph represents information on an individual association test. The color is indicative of the direction and magnitude of the effect, while the shape itself indicates the p-value bin

Association tests were performed for six neuropathological phenotypes, all rendering significant signals as expected based on the previous results (Fig. 2). P-values remained in the same order of magnitude for most phenotypes except for CAA severity ($p = 0.003$, $\beta = 0.31$, SE = 0.1) and Aβ score ($p = 0.0007$, $\beta = 0.47$, SE = 2.7) where the signal was stronger using hard-called genotypes compared to dosages. For Braak NFT stage ($p = 5 \times 10^{-07}$, $\beta = 0.83$, SE = 0.16), CERAD score ($p = 0.0003$, $\beta = 0.38$, SE = 0.1), GVD stage ($p = 0.0003$, $\beta = 0.07$, SE = 0.02), ABC neuropathological score ($p = 1.8 \times 10^{-05}$, $\beta = 0.45$, SE = 0.1) and Aβ score, there was a clear increase in the level of pathology with each T allele for rs117618017 where homozygous SNP carriers generally had the highest levels of pathology. Only for the CAA severity score, the group of individuals which were heterozygous for the SNP seemed to have higher levels of pathology compared to either homozygous genotype groups.

Additional statistical models were used portraying the relation between pTau, Aβ, *APH1B* genotype and age at death to model the directionality of the effects observed in the initial analysis. First, regression models were constructed implementing Braak NFT and Aβ score as covariates. When

Table 2 Association between 75 AD risk SNPs and 12 neuropathological phenotypes

Phenotype	Chr	Variant ID	Gene	REF	ALT	Effect	Beta/OR	L95	U95	*P* value	R^2
Braak NFT ($n=325$)	19	rs429358	*APOE*	T	C	C	0.75	0.47	1.02	$\mathbf{1.58\times10^{-07}}$	0.100
	15	rs117618017	*APH1B*	C	T	T	0.87	0.53	1.20	$\mathbf{6.90\times10^{-07}}$	0.047
	8	rs73223431	*PTK2B*	C	T	T	0.31	0.09	0.53	0.005	0.024
	3	rs16824536	*MME*	G	A	G	0.67	− 1.19	− 0.14	0.013	0.026
	19	rs7412	*APOE*	C	T	T	− 0.48	− 0.91	− 0.04	0.032	0.005
	4	rs3822030	*IDUA*	G	T	T	0.25	− 0.47	− 0.02	0.033	0.025
	19	rs9304690	*SIGLEC11*	C	T	T	0.29	0.02	0.56	0.037	0.010
Aβ score ($n=324$)	19	rs429358	*APOE*	T	C	C	1.01	0.74	1.28	$\mathbf{1.71\times10^{-12}}$	0.155
	19	rs7412	*APOE*	C	T	T	− 0.88	− 1.31	− 0.45	$\mathbf{7.22\times10^{-05}}$	0.031
	11	rs3851179	*EED*	T	C	T	− 0.34	− 0.58	− 0.10	0.005	0.014
	1	rs679515	*CR1*	T	C	T	0.37	0.09	0.65	0.009	0.037
	15	rs117618017	*APH1B*	C	T	T	0.44	0.09	0.79	0.015	0.011
	21	rs2830489	*ADAMTS1*	C	T	T	0.28	0.03	0.52	0.026	0.018
CERAD ($n=325$)	19	rs429358	*APOE*	T	C	C	0.48	0.31	0.65	$\mathbf{8.04\times10^{-08}}$	0.105
	15	rs117618017	*APH1B*	C	T	T	0.38	0.17	0.59	**0.0005**	0.028
	8	rs73223431	*PTK2B*	C	T	T	0.23	0.09	0.36	0.001	0.033
	19	rs7412	*APOE*	C	T	T	− 0.35	− 0.62	− 0.08	0.011	0.013
	20	rs6742	*SLC2A4RG*	T	C	C	− 0.20	0.03	0.36	0.02	0.013
	21	rs2830489	*ADAMTS1*	C	T	C	− 0.17	0.02	0.31	0.032	0.018
	7	rs13237518	*TMEM106B*	C	A	C	0.15	− 0.28	− 0.01	0.039	0.015
Braak PD ($n=321$)	7	rs6943429	*UMAD1*	T	C	T	0.40	0.14	0.65	0.003	0.028
	2	rs6733839	*BIN1*	C	T	T	0.41	0.12	0.70	0.005	0.022
	10	rs7912495	*USP6NL*	A	G	G	0.36	0.10	0.63	0.008	0.023
	19	rs429358	*APOE*	T	C	C	0.38	0.04	0.73	0.030	0.023
	20	rs6742	*SLC2A4RG*	T	C	T	0.36	0.03	0.68	0.031	0.009
	15	rs3848143	*SNX1*	G	A	G	0.37	0.03	0.70	0.034	0.015
α-synuclein in CA1 ($n=321$)	19	rs429358	*APOE*	T	C	C	1.77	1.13	2.75	0.012	0.026
	17	rs7225151	*SCIMP*	G	A	A	1.90	1.13	3.18	0.015	0.021
	7	rs6943429	*UMAD1*	T	C	T	1.54	1.08	2.19	0.018	0.017
	15	rs3848143	*SNX1*	G	A	G	1.57	1.01	2.43	0.045	0.139
α-synuclein beyond brainstem ($n=321$)	10	rs7912495	*USP6NL*	A	G	G	2.03	1.24	3.32	0.005	0.026
	2	rs6733839	*BIN1*	C	T	T	1.97	1.17	3.31	0.011	0.017
	19	rs429358	*APOE*	T	C	C	1.89	1.11	3.22	0.020	0.028
	7	rs6943429	*UMAD1*	T	C	T	1.71	1.09	2.70	0.021	0.017
	2	rs17020490	*PRKD3*	T	C	C	2.00	1.02	3.91	0.044	0.008
	20	rs6742	*SLC2A4RG*	T	C	T	1.75	1.01	3.02	0.044	0.007
LATE-NC ($n=233$)	10	rs7068231	*ANK3*	T	G	T	− 0.18	− 0.31	− 0.06	0.004	0.036
	16	rs450674	*MAF*	T	C	C	0.19	0.05	0.32	0.006	0.023
	19	rs429358	*APOE*	T	C	C	0.19	0.04	0.35	0.017	0.035
	12	rs6489896	*TPCN1*	T	C	C	0.32	0.06	0.57	0.017	0.036

Table 2 (continued)

Phenotype	Chr	Variant ID	Gene	REF	ALT	Effect	Beta/OR	L95	U95	*P* value	R^2
	10	rs6586028	*TSPAN14*	C	T	C	− 0.19	− 0.36	− 0.03	0.021	0.024
	2	rs6733839	*BIN1*	C	T	T	0.16	0.02	0.30	0.022	0.021
	15	rs117618017	*APH1B*	C	T	T	0.20	0.02	0.39	0.034	0.010
	19	rs7412	*APOE*	C	T	T	− 0.26	− 0.51	− 0.01	0.045	0.011
pTDP-43 in CA1 ($n=321$)	19	rs429358	*APOE*	T	C	C	2.05	1.23	3.41	0.006	0.035
	10	rs7068231	*ANK3*	T	G	T	0.54	0.33	0.89	0.015	0.019
	20	rs6742	*SLC2A4RG*	T	C	T	0.43	0.22	0.86	0.016	0.016
	2	rs6733839	*BIN1*	C	T	T	1.78	1.09	2.90	0.021	0.015
	9	rs1800978	*ABCA1*	C	G	G	2.00	1.04	3.87	0.038	0.013
	2	rs72777026	*ADAM17*	A	G	G	1.87	1.02	3.42	0.042	0.012
pTDP-43 in dentate gyrus ($n=313$)	20	rs6742	*SLC2A4RG*	T	C	T	0.21	0.08	0.58	0.002	0.032
	9	rs1800978	*ABCA1*	C	G	G	2.44	1.18	5.02	0.016	0.018
	2	rs6733839	*BIN1*	C	T	T	1.94	1.12	3.36	0.019	0.018
	10	rs7068231	*ANK3*	T	G	T	0.55	0.32	0.96	0.035	0.014
	6	rs143332484	*TREM2*	C	T	T	5.17	1.09	24.60	0.039	0.012
GVD stage ($n=319$)	19	rs429358	*APOE*	T	C	C	0.49	0.22	0.75	**0.0003**	0.057
	15	rs117618017	*APH1B*	C	T	T	0.57	0.25	0.90	0.0007	0.022
	19	rs7412	*APOE*	C	T	T	− 0.56	− 0.97	− 0.15	0.008	0.010
	21	rs2830489	*ADAMTS1*	C	T	T	0.27	0.04	0.50	0.021	0.023
	8	rs73223431	*PTK2B*	C	T	T	0.22	0.02	0.43	0.035	0.014
CAA ($n=325$)	19	rs429358	*APOE*	T	C	C	0.55	0.38	0.71	$\mathbf{3.84\times10^{-10}}$	0.133
	15	rs117618017	*APH1B*	C	T	T	0.28	0.07	0.49	0.010	0.017
	6	rs7767350	*CD2AP*	C	T	T	− 0.17	− 0.32	− 0.02	0.024	0.022
ABC score ($n=325$)	19	rs429358	*APOE*	T	C	C	0.63	0.46	0.79	$\mathbf{1.12\times10^{-12}}$	0.165
	19	rs7412	*APOE*	C	T	T	− 0.60	− 0.86	− 0.33	$\mathbf{1.30\times10^{-05}}$	0.037
	15	rs117618017	*APH1B*	C	T	T	0.42	0.21	0.63	**0.0001**	0.029
	21	rs2830489	*ADAMTS1*	C	T	C	− 0.19	0.04	0.34	0.014	0.021
	17	rs4277405	*ACE*	C	T	T	0.16	− 0.30	− 0.01	0.034	0.016
	11	rs3851179	*EED*	T	C	C	0.16	− 0.30	− 0.01	0.035	0.008
	20	rs6742	*SLC2A4RG*	T	C	C	− 0.17	0.01	0.34	0.044	0.008
	8	rs73223431	*PTK2B*	C	T	T	0.14	0.002	0.28	0.047	0.014

Results of the regression models are summarized here. For each phenotype that was investigated, all hits reaching nominal significance of $p<0.05$ are shown, as well as information regarding the chromosome, variant ID, the prioritized gene in the variant region following Bellenguez et al., the reference allele, alternative allele, and the effect allele, as well as total sample size per phenotype and the variance explained for each phenotype-genotype relation (R^2). Of note, LATE-NC staging was not performed for ALS and FTLD cases. Effect sizes/ORs and standard errors are described as well. The p-values marked in bold are passing Bonferroni multiple testing correction ($p<0.0006$) and were considered as the significant association discovered in this study

Table 3 Top associated SNPs for which concordance was checked with Oxford Nanopore sequencing

rsID SNP	Chromosome	Genomic position	Minor allele	Major allele	MAF	Concordance	Gene
rs117618017	15	63,277,703	T	C	0.12	97.50	*APH1B*
rs429358	19	44,908,684	C	T	0.16	99.70	*APOE*
rs7412	19	44,908,822	T	C	0.07	99.70	*APOE*

Minor allele frequencies (MAF) reported here are calculated based on allele frequencies observed in the low-coverage whole-genome sequencing dataset

rsID reference SNP identifier

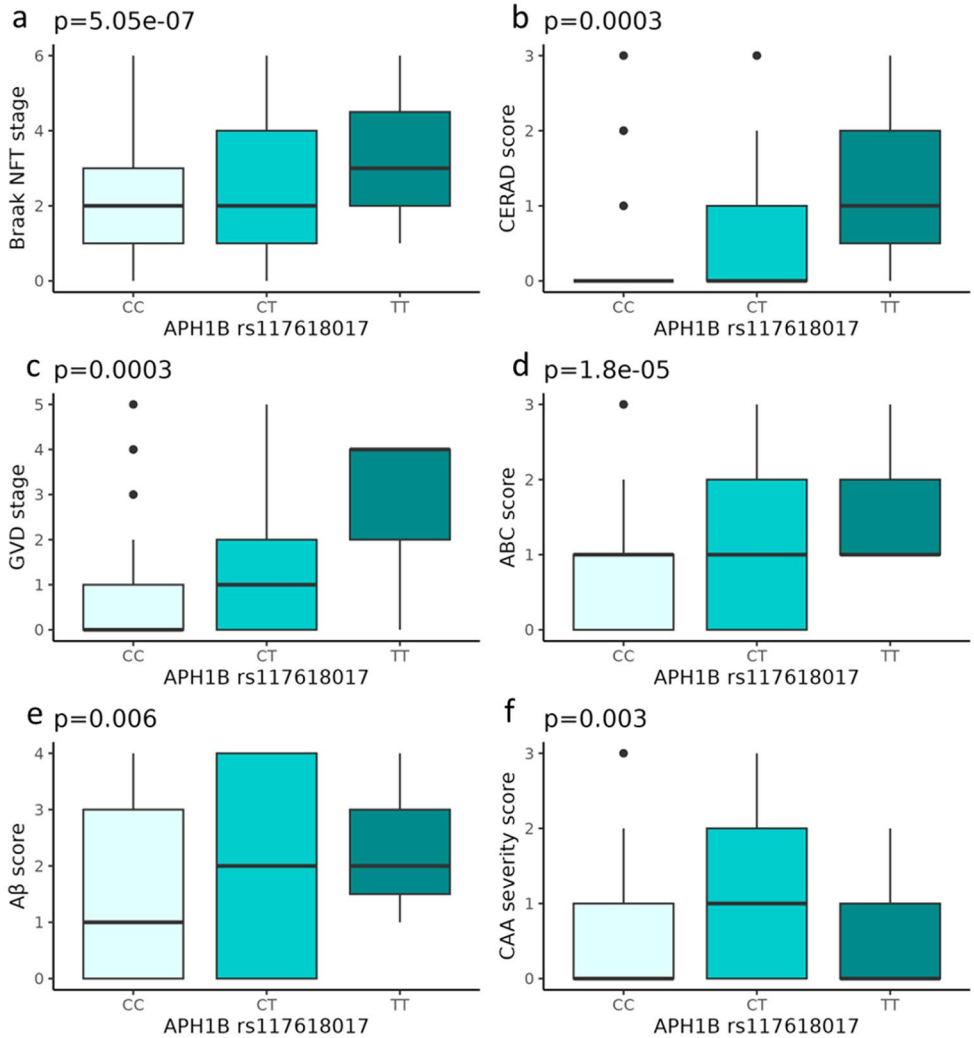

Fig. 2 *APH1B* association with neuropathological phenotypes. Panel **A**–**F**; Panels show boxplots for Braak NFT stage, CERAD neuritic plaque score, GVD stage, ABC score, Aβ score and CAA severity respectively. The y-axis represents the stage or score of the phenotype and the *x*-axis represents the genotype for rs117618017

constructing the model investigating association between pTau and rs117618017 (*APH1B*), using Aβ score as a covariate, there is a persisting significant effect ($p = 1.24 \times 10–05$, $\beta = 0.58$, SE = 0.13). On the other hand, for the regression model investigating the relation with Aβ, including Braak NFT stage as a covariate omits the significant signal ($p = 0.64$, $\beta = -0.07$, SE = 0.14). The disappearance of the effect of Aβ when correcting for pTau is an indication that the relation with rs117618017 is likely not direct but rather modulated by pTau.

To further explore the connection between neuropathological lesions and AD risk SNPs, a graphical lasso model was constructed for $n=267$ individuals who had phenotyping data available for age at death, Braak NFT, Aβ score and GVD stage (Fig. 3). Additionally, the two SNPs for which significant associations with these neuropathological phenotypes were discovered, were also included in the model. This network approach revealed nine edges, each indicating a positive dependency between nodes (i.e., variables). The strongest dependency in the network was observed between GVD stage and Braak NFT stage ($r=0.48$). Braak NFT stage also had an edge with the age at death ($r=0.1$). There were also edges connecting GVD stage with Aβ score ($r=0.17$) and age at death ($r=0.13$). The second strongest dependency was observed between Aβ score and Braak NFT stage ($r=0.33$). Finally, the genetic factors included in this model, rs117618017 (APH1B) and rs429358 (APOE) showed a positive dependency with Braak NFT stage ($r=0.11$) and Aβ score ($r=0.17$) respectively. Between rs429358 and Braak NFT stage, there was a small dependency as well ($r=0.06$). From this graphical network, it became apparent that the relation that was discovered between *APOE* SNP rs429358 and GVD stage is likely not a direct association but is modulated by Aβ pathology and pTau since there is no direct edge connecting *APOE* to GVD. On the other hand, the association discovered between *APH1B* SNP rs117618017 and pTau seems to be a direct effect, where the association between rs117618017 and Aβ seems to be modulated through pTau. These results complement our hypothesis that the effect of rs117618017 on pTau is a direct effect while the effect on Aβ is mainly mediated through pTau. Model stability was validated using bootstrapping and the CS-coefficient. Results showed that the model is robust with CS coefficients for both node strength and edge weights being 0.752, indicating the model metrics remaining stable when up to 75.2% of the data was dropped, implicating reliability of the model.

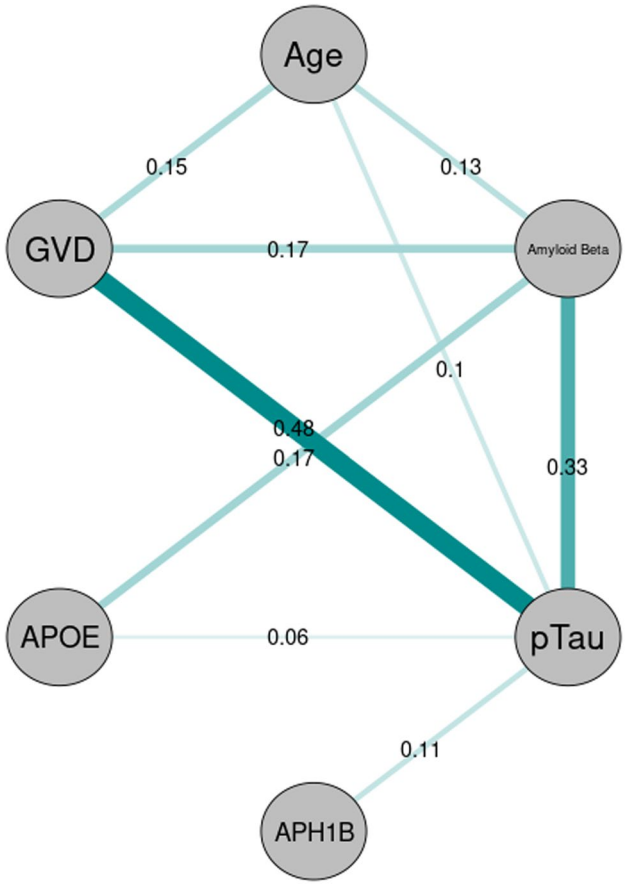

Fig. 3 Network analysis. A graphical network constructed employing a graphical lasso model. Every edge (i.e., line) that connects two nodes (i.e., variables) represents a positive conditional dependency between those variables. The strength of the dependency is represented by the width of the edge and the *r* value, which is displayed at the center of every edge. From this graphical representation, the interaction between different risk factors can be deduced. Relevant to this study is the direct dependency between rs117618017 and pTau (Braak NFT), indirect dependency between rs117618017 and Aβ (Aβ score) and the indirect dependency between rs429358 and Aβ

Meta-analysis using three independent cohorts

In order to investigate the robustness of the significant and subthreshold associations discovered in this study, a meta-analysis was performed utilizing published summary statistics on ADSP, ADGC and ROSMAP cohorts [36] for four neuropathological traits for which phenotypes could be harmonized: neuritic plaques (CERAD), pTau (Braak NFT), pTDP and α-synuclein. Of note, scores for Braak NFT, CERAD and the three TDP phenotypes were converted to binary phenotypes in the Leuven Brain Collection to enable this meta-analysis. All results of the meta-analysis are summarized in Table 4. For some variants, summary statistics were only available in some of the cohorts. Therefore, information about the specific cohorts and sample sizes analyzed for every genotype–phenotype combination is indicated. Meta-analysis confirmed the association between *APH1B* and pTau pathology ($p=0.001$) and neuritic plaques ($p=0.0002$) with the same directionality as observed in the discovery cohort. Additionally, several of the sub threshold associations of the discovery cohort were confirmed in the meta-analysis: *PTK2B* was significantly associated with pTau pathology ($p=0.002$) and neuritic plaques ($p=0.0006$). *MME* was significantly associated with pTau pathology ($p=0.0006$). Regarding pTDP pathology, several variants had nominally significant p-values in the meta-analysis, including *TPCN1* ($p=0.001$). Finally, significant association was observed between α-synuclein pathology and *BIN1* ($p=0.0006$).

Table 4 Meta-analysis of variants with at least one nominal significant association in the discovery analysis

Gene	rsID	Effect allele	Leuven Brain Collection		ADSP		ADGC		ROSMAP		Meta-analysis	
			OR	*P* value	OR	*P* value	OR	*P* value	OR	*P* value	*Z* score	*P* value
pTau pathology			*n* = 325		*n* = 1026		*n* = 2191		*n* = 1266			
SIGLEC11	rs9304690	T	2.01	0.02	0.94	0.62	0.99	0.91	1	0.99	0.90	0.37
PTK2B	rs73223431	T	2.24	0.002	0.98	0.86	1.1	0.17	1.25	0.015	3.07	0.0021
APH1B	rs117618017	T	4.34	0.0001	1.07	0.65	1.08	0.43	1.45	0.0042	3.23	0.0012
MME	rs16824536	A	0.34	0.30	0.54	0.01	0.65	0.0038	1	0.99	3.44	0.0006
Neuritic plaques			*n* = 325		*n* = 1028		*n* = 2195		*n* = 1266			
PTK2B	rs73223431	T	3.17	0.0004	1.14	0.2	1.09	0.23	1.21	0.029	3.45	0.0006
APH1B	rs117618017	T	3.31	0.006	1.05	0.73	1.24	0.026	1.38	0.01	3.70	0.0002
ADAMTS1	rs2830489	T	2.67	0.003	1.08	0.47	1.05	0.49	0.92	0.36	2.03	0.04
SLC2A4RG	rs6742	T	2.26	0.02	1.04	0.72	1.03	0.73	1.06	0.57	1.30	0.20
TMEM106B	rs13237518	A	0.40	0.02	1.07	0.49	1	0.95	0.92	0.35	1.46	0.14
pTDP pathology			*n* = 313		*n* = 364		*n* = 797		*n* = 1176			
TREM2	rs143332484	T	2.33	0.28	0.8	0.77	NA	NA	NA	NA	0.94	0.35
TSPAN14	rs6586028	T	0.63	0.12	NA	NA	0.94	0.66	0.91	0.41	− 1.42	0.16
ABCA1	rs1800978	C	1.56	0.16	NA	NA	NA	NA	1.22	0.13	− 1.99	0.05
TPCN1	rs6489896	T	2.05	0.06	1.72	0.09	1.05	0.84	1.63	0.0069	− 3.17	0.0015
BIN1	rs6733839	T	2.08	0.001	1.05	0.78	1.11	0.33	1.02	0.83	1.87	0.06
SLC2A4RG	rs6742	T	0.44	0.008	1.39	0.13	0.97	0.83	1.02	0.83	2.68	0.0073
ADAM17	rs72777026	A	1.61	0.10	0.88	0.6	1.06	0.71	1.19	0.099	− 1.61	0.11
MAF	rs450674	T	1.25	0.31	NA	NA	0.91	0.4	1.1	0.28	− 1.65	0.10
ANK3	rs7068231	T	0.51	0.003	1.19	0.37	0.92	0.42	0.96	0.6	2.14	0.03
A-synuclein pathology			*n* = 321		*n* = 1023		*n* = 2185		*n* = 1225			
PRKD3	rs17020490	T	1.67	0.06	1.14	0.29	0.97	0.71	0.9	0.44	− 1.62	0.10
USP6NL	rs7912495	A	1.32	0.14	1.08	0.45	1.12	0.069	1.26	0.021	− 3.14	0.0017
SNX1	rs3848143	A	1.52	0.06	1.12	0.31	0.86	0.06	1.02	0.86	− 2.32	0.02
BIN1	rs6733839	T	1.28	0.22	1.24	0.02	1.13	0.054	1.16	0.13	3.45	0.0006
SLC2A4RG	rs6742	T	1.51	0.06	0.98	0.89	1.03	0.73	1.02	0.89	0.85	0.40
SCIMP	rs7225151	A	1.79	0.03	1.1	0.49	1.26	0.017	0.95	0.75	2.68	0.0074
UMAD1	rs6943429	T	1.54	0.02	0.84	0.08	0.99	0.93	0.95	0.75	1.74	0.08

Meta-analysis performed on harmonized neuropathology traits in Leuven Brain Collection, ADSP, ADGC and ROSMAP cohorts. Z-scores and p-values are reported as well as the effect allele. For this meta-analysis, neuropathology scores for Braak NFT and CERAD were converted to a binary phenotype in the Leuven Brain Collection, and the three TDP-related traits in the Leuven Brain Collection were converted into a single binary trait reflecting pTDP pathology to enable meta-analysis, which results in some SNP-trait associations in the Leuven Brain Collection not fully matching the discovery analysis which was performed on semi-quantitative phenotypes. For every cohort used in the meta-analysis, Odds ratio (OR) and p-value are reported. P-values of 0.002 and lower are passing Bonferroni correction for the number of SNP-phenotype associations tested in the meta-analysis

Discussion

We investigated the relation between known AD risk SNPs and neuropathological lesions in the Leuven Brain Collection, a novel, deeply characterized post-mortem brain cohort. We observed significant association between *APH1B* and pTau-related phenotypes. Additionally, nominal significant associations were observed between *APH1B* and GVD, CAA and Aβ pathology. *APOE* showed associations with hallmark AD lesions, as well as with granulovacuolar degeneration. Numerous subthreshold associations were observed, several of which were substantiated by meta-analysis with three independent cohorts, revealing potentially interesting associations between AD risk genes and non-AD neuropathologies, such as *BIN1* and α-synuclein pathology.

The connection between *APOE* and Aβ pathology is well-studied and is very likely a direct effect, with *APOE* ε4 contributing to the pathogenesis by for example inducing Aβ oligomerization [68]. The association we observed between GVD and *APOE* is in contrast with earlier work, investigating human autopsy brains for the relation between LATE-NC, GVD and pTau. This study reported no association between *APOE* and GVD [37]. A possible explanation for this discrepancy could be the lower power of that study to detect significant genetic associations due to a limited sample size. In our study, accurate genotype and phenotype data for GVD were available for 319 individuals, substantially increasing the power to detect smaller effects compared to earlier work. Network analysis however indicated that the effect of *APOE* on GVD might not be direct, but rather mediated by Aβ pathology. This warrants further investigation into the relation between the *APOE* genotype and GVD to better comprehend how they are interacting in AD pathology. To validate these findings, replication of the associations in an independent cohort is needed, but the lack of deeply phenotyped neuropathological cohorts, especially for less-studied lesions such as GVD, is a substantial limitation. Therefore, some caution is warranted in the interpretation of these findings.

Besides *APOE*, the AD risk gene *APH1B* came forward in this study with significant associations with Braak NFT stage, CERAD score and ABC score in the Leuven Brain Collection. Additionally, trends toward significance were observed for GVD stage, LATE-NC, CAA and Aβ score. The association with Braak NFT stage and CERAD score was observed as a subthreshold association in an independent study [36]. When we meta-analyzed our results with this independent dataset in total meta-analysis sample sizes of 4808 and 4814 respectively, the associations persisted. *APH1B* encodes a multi-pass transmembrane protein which is a stabilizing subunit of the γ-secretase protein complex. Γ-secretase comprises four subunits: presenilin (PS1 and PS2 homologs), nicastrin, anterior pharynx-defective 1 (APH-1) and presenilin enhancer two [15]. In humans, the two physiological isoforms of APH-1 are APH1A and APH1B. The structural heterogeneity of the isoforms exerts a main effect on the carboxypeptidase activity of γ-secretase, where complexes containing APH1B are less efficient compared to APH1A [1]. Additionally, APH1B containing complexes tend to generate longer, more toxic Aβ species upon cleavage of the most well-known γ-secretase substrate, APP [54]. Due to the well-established function of γ-secretase in APP cleavage, it would be expected that there is a stronger relation between the AD risk SNP in *APH1B* and Aβ-related phenotypes. However, in this study, the evidence points more toward a relation with tau-related pathologies when directionality of the effect was investigated using Braak NFT and Aβ score as covariates in a regression model and by subsequent construction of a graphical network. Both analyses indicated a direct relation between *APH1B* rs117618017 and tau pathology rather than Aβ pathology. It can be hypothesized that the effect on tau pathology is exerted through the APP intracellular domain (AICD) rather than through Aβ peptides, as both co-localize in the nucleus of cell where AICD could interact with tau through modulation of the DNA binding capacity and DNA protective function [46]. A study has also shown a relation between tau and AICD in a transgenic AICD mouse model, where ablation of tau seemed protective for AD-like features, indicating that tau is crucial in mediation of the deleterious effects of AICD [22]. Evidence has also been gathered regarding the relation of other γ-secretase subunits with tau pathology, such as presenilin. In mouse models, partial loss of the presenilin subunit resulted in tau aggregation and phosphorylation, increasing overall neurodegeneration [55]. Supporting this relation is the evidence linking presenilin mutations to other tauopathies, such as frontotemporal dementia [8, 52] and Pick's disease [16]. Additionally, APP metabolism has also been linked to tau proteostasis in cell culture models [45], possibly through regulation of endosome/lysosomal pathways [9]. Interestingly, recent work has also linked an AD risk missense mutation in SORL1, a transmembrane, endosomal protein involved in APP trafficking to tau by showing colocalization in cell lines as well as mediation of tau seeding by mutant SORL1 [13]. This further strengthens the possibility of a relation between γ-secretase, and thus APH1B, to tau pathology.

Rs117618017, encoding a missense mutation in the APH1B protein, has a robust association with clinical AD with evidence compiled from multiple genome-wide association studies and meta-analyses [31, 67]. Using imaging biomarkers, altered expression levels in blood of APH1B

RNA have also been linked to amyloid PET and brain atrophy [51], further emphasizing the importance of *APH1B* in AD pathology. However, this study only focused on markers for Aβ pathology or neurodegeneration and did not investigate the possible relation of *APH1B* to tau pathology. Functional studies have also investigated the involvement of *APH1B* in AD. One study expressed the variant in cell lines and reported no significant effects on APP cleavage [70], suggesting that the effect observed here is possibly not directly attributable to the cleave of APP although further investigation is needed. Here, it is proposed that the T allele at rs117618017 increases tau-related pathology, likely through an overall increase of APH1B levels although functional validation experiments are needed to identify the true mechanism of action.

Finally, we observed several subthreshold associations in the discovery cohort, which persisted in the meta-analysis. This includes an association between *BIN1* and α-synuclein pathology. Of interest, a whole-genome sequencing study on LBD previously reported a genome-wide association between the *BIN1* locus and risk for LBD with the same directionality of effect as observed in AD [12]. In contrast, however, a study investigating the genetic risk of AD cases with and without Lewy body pathology reported that *BIN1* risk was associated with AD pathology rather than Lewy body pathology [58]. Further studies are needed to elucidate the potential role of *BIN1* in α-synuclein pathology. Additionally, we observed nominal association for *UMAD1* and *USP6NL* with α-synuclein pathology. The latter was also suggested by a prior study [36] and was replicated in our meta-analysis. Meta-analysis did also confirm the association between *PTK2B* and pTau pathology and neuritic plaques. The *PTK2B* protein product, Pyk2, has been suggested to be involved in tau toxicity in animal models [17, 24, 42] and the *PTK2B* risk allele was also associated with longitudinal increase of CSF pTau levels in humans [60]. Finally, meta-analysis confirmed an association between *TPCN1* and pTDP pathology, while also showing nominal associations for *SLC2A4RG* and *ANK3*. Intriguingly, TDP43 expression seemed to trigger an increase in the expression of ANK3 in a human iPSC model of ALS [25]. We did not detect associations with specific TDP-related risk genes, like *GRN* and *TMEM106B*, which could in part be due to the sample size of this study or due to low number of FTLD/ALS cases in our cohort.

Conclusion

Genome-wide association studies rapidly discover genetic variants linked to the clinical diagnosis of AD, but there is a need for studies expanding on these findings to understand which variants are at play in what part of the heterogeneous pathological spectrum of AD. Here, we reported first evidence that genetic variation in the γ-secretase component *APH1B* is associated with tau pathology. Additionally, a relation between *APOE* and granulovacuolar degeneration was observed. This effect was proven to be likely indirect through Aβ and pTau, providing accumulating evidence for the relation between *APOE* and hallmark AD pathology. The results obtained from this investigation offer an opportunity to gain insights into how AD risk variants are exactly involved in AD pathology, more specifically, where certain genetic variants can be mapped to specific neuropathological lesions observed along the AD spectrum.

Supplementary Information The online version contains supplementary material available at https://doi.org/10.1007/s00401-024-02815-w.

Acknowledgements This work was supported by the Fund for Scientific Research Flanders (KS,DRT:FWO G065721N), KU-Leuven Onderzoeksraad (PVD, DRT: C14/22/132) and Alzheimer Association/ USA (DRT: grant No. 22-AAIIA-963171). SOT is supported by a BrightFocus Foundation Fellowship Grant (A2022019F). FK is recipient of a postdoctoral fellowship (BOF 49758) of the Special Research Fund of the University of Antwerp. ROSMAP WGS: The results published here are in whole or in part based on data obtained from the AD Knowledge Portal (https://adknowledgeportal.org). Study data were provided by the Rush Alzheimer's Disease Center, Rush University Medical Center, Chicago. Data collection was supported through funding by NIA grants P30AG10161 (ROS), R01AG15819 (ROSMAP; genomics and RNAseq), R01AG17917 (MAP), R01AG30147, R01AG36042 (5hC methylation, ATACseq), RC2AG036547 (H3K9Ac), R01AG36836 (RNAseq), R01AG48015 (monocyte RNAseq) RF1AG57473 (single nucleus RNAseq), U01AG32984 (genomic and whole exome sequencing), U01AG46152 (ROSMAP AMP-AD, targeted proteomics), U01AG46161(TMT proteomics), U01AG61356 (whole-genome sequencing, targeted proteomics, ROSMAP AMP-AD), the Illinois Department of Public Health (ROSMAP), and the Translational Genomics Research Institute (genomic). Additional phenotypic data can be requested at www.radc.rush.edu.

Funding The funding has been received from Fund for Scientific Research Flanders with Grant no. FWO G065721N; FWO with Grant no. FWO G065721N; Onderzoeksraad, KU Leuven with Grant no. C14/22/132; Alzheimer's Association with Grant no. 22-AAIIA-963171; BrightFocus Foundation with Grant no. A2022019F; BOF UAntwerp with Grant no. 49758.

Data availability All relevant data are provided in the tables of the paper, so an additional data availability is redundant.

Declarations

Conflict of interest DRT collaborated with Novartis Pharma AG (Switzerland), Probiodrug (Germany), GE-Healthcare (UK), and Janssen Pharmaceutical Companies (Belgium). DRT and KS are members of Acta Neuropathologica editorial board. They were not involved in the assessment or decision-making process for this manuscript. CAF-vA received honoraria from serving on the scientific advisory board of Biogen, Roche, Novo Nordisk, Biontech, Lilly, Dr. Willmar Schwabe GmbH &Co. KG, and MindAhead UG and has received funding for travel and speaker honoraria from Biogen, Lilly, Novo Nordisk, Roche diagnostics AG, Novartis, Medical Tribune Verlagsgesellschaft mbH, Landesvereinigung für Gesundheit und Akademie für Sozialmedizin Niedersachsen e. V., FomF GmbH | Forum für medizinische Fortbil-

dung and Dr. Willmar Schwabe GmbH &Co. KG has received research support from Roche diagnostics AG. RVs institution has clinical trial agreements (RV as PI) with Alector, Biogen, Denali, J&J, EliLilly, and UCB and consultancy agreements (RV as DSMB member) with AC Immune. The other authors have nothing to disclose.

Ethical approval Tissue collection was performed in accordance with the local ethical committee guidelines and laws regarding the use of human tissue for research. The research protocol for the current study was approved by the ethical committees of the UZ/KU Leuven and UZA/University of Antwerp.

References

1. Acx H, Chávez-Gutiérrez L, Serneels L, Lismont S, Benurwar M, Elad N et al (2014) Signature amyloid β profiles are produced by different γ-secretase complexes*. JBC 289:4346–4355. https://doi.org/10.1074/jbc.M113.530907
2. Alafuzoff I, Pikkarainen M, Al-Sarraj S, Arzberger T, Bell J, Bodi I et al (2006) Interlaboratory comparison of assessments of Alzheimer disease-related lesions: a study of the BrainNet Europe Consortium. J Neuropathol Exp Neurol 65:740–757. https://doi.org/10.1097/01.jnen.0000229986.17548.27
3. Arslan S, Garcia FJ, Guo M, Kellinger MW, Kruglyak S, LeVieux JA et al (2024) Sequencing by avidity enables high accuracy with low reagent consumption. Nat Biotechnol 42:132–138. https://doi.org/10.1038/s41587-023-01750-7
4. Auton A, Abecasis GR, Altshuler DM, Durbin RM, Abecasis GR, Bentley DR et al (2015) A global reference for human genetic variation. Nature 526:68–74. https://doi.org/10.1038/nature15393
5. Bellenguez C, Küçükali F, Jansen IE, Kleineidam L, Moreno-Grau S, Amin N et al (2022) New insights into the genetic etiology of Alzheimer's disease and related dementias. Nat Genet 54:412–436. https://doi.org/10.1038/s41588-022-01024-z
6. Bennett DA, Buchman AS, Boyle PA, Barnes LL, Wilson RS, Schneider JA (2018) Religious orders study and rush memory and aging project. J Alzheimers Dis 64:S161-s189. https://doi.org/10.3233/jad-179939
7. Bergem AL, Engedal K, Kringlen E (1997) The role of heredity in late-onset Alzheimer disease and vascular dementia. A twin study. Arch Gen Psychiatry 54:264–270. https://doi.org/10.1001/archpsyc.1997.01830150090013
8. Bernardi L, Tomaino C, Anfossi M, Gallo M, Geracitano S, Costanzo A et al (2009) Novel PSEN1 and PGRN mutations in early-onset familial frontotemporal dementia. Neurobiol Aging 30:1825–1833. https://doi.org/10.1016/j.neurobiolaging.2008.01.005
9. Bourdenx M, Martín-Segura A, Scrivo A, Rodriguez-Navarro JA, Kaushik S, Tasset I et al (2021) Chaperone-mediated autophagy prevents collapse of the neuronal metastable proteome. Cell J 184:2696-2714.e2625. https://doi.org/10.1016/j.cell.2021.03.048
10. Braak H, Alafuzoff I, Arzberger T, Kretzschmar H, Del Tredici K (2006) Staging of Alzheimer disease-associated neurofibrillary pathology using paraffin sections and immunocytochemistry. Acta Neuropathol 112:389–404. https://doi.org/10.1007/s00401-006-0127-z
11. Braak H, Tredici KD, Rüb U, de Vos RAI, Jansen Steur ENH, Braak E (2003) Staging of brain pathology related to sporadic Parkinson's disease. Neurobiol Aging 24:197–211. https://doi.org/10.1016/S0197-4580(02)00065-9
12. Chia R, Sabir MS, Bandres-Ciga S, Saez-Atienzar S, Reynolds RH, Gustavsson E et al (2021) Genome sequencing analysis identifies new loci associated with Lewy body dementia and provides insights into its genetic architecture. Nat Genet 53:294–303. https://doi.org/10.1038/s41588-021-00785-3
13. Cooper JM, Lathuiliere A, Su EJ, Song Y, Torrente D, Jo Y et al (2024) SORL1 is a receptor for tau that promotes tau seeding. J Biol Chem 300:107313. https://doi.org/10.1016/j.jbc.2024.107313
14. Crane PK, Foroud T, Montine TJ, Larson EB (2017) Alzheimer's disease sequencing project discovery and replication criteria for cases and controls: data from a community-based prospective cohort study with autopsy follow-up. Alzheimers Dement 13:1410–1413. https://doi.org/10.1016/j.jalz.2017.09.010
15. De Strooper B (2003) Aph-1, Pen-2, and Nicastrin with Presenilin generate an active gamma-Secretase complex. Neuron 38:9–12. https://doi.org/10.1016/s0896-6273(03)00205-8
16. Dermaut B, Kumar-Singh S, Engelborghs S, Theuns J, Rademakers R, Saerens J et al (2004) A novel presenilin 1 mutation associated with Pick's disease but not beta-amyloid plaques. Ann Neurol 55:617–626. https://doi.org/10.1002/ana.20083
17. Dourlen P, Fernandez-Gomez FJ, Dupont C, Grenier-Boley B, Bellenguez C, Obriot H et al (2017) Functional screening of Alzheimer risk loci identifies PTK2B as an in vivo modulator and early marker of Tau pathology. Mol Psychiatry 22:874–883. https://doi.org/10.1038/mp.2016.59
18. Edge P, Bansal V (2019) Longshot enables accurate variant calling in diploid genomes from single-molecule long read sequencing. Nat Commun 10:4660. https://doi.org/10.1038/s41467-019-12493-y
19. Epskamp S, Borsboom D, Fried EI (2018) Estimating psychological networks and their accuracy: a tutorial paper. Behav Res Methods 50:195–212. https://doi.org/10.3758/s13428-017-0862-1
20. Foygel R, Drton M (2010) Extended Bayesian information criteria for Gaussian graphical models. In: Proceedings of the 23rd International Conference on Neural Information Processing Systems—Volume 1. Curran Associates Inc., City, pp 604–612
21. Friedman J, Hastie T, Tibshirani R (2008) Sparse inverse covariance estimation with the graphical lasso. J Biostat 9:432–441. https://doi.org/10.1093/biostatistics/kxm045
22. Ghosal K, Fan Q, Dawson HN, Pimplikar SW (2016) Tau protein mediates APP intracellular domain (AICD)-induced Alzheimer's-like pathological features in mice. PLoS ONE 11:e0159435. https://doi.org/10.1371/journal.pone.0159435
23. Hamilton RL (2000) Lewy bodies in Alzheimer's disease: a neuropathological review of 145 cases using α-synuclein immunohistochemistry. Brain Pathol 10:378–384. https://doi.org/10.1111/j.1750-3639.2000.tb00269.x
24. Hao KM, Liu Z, Wang HY, Qi WX (2022) Time dependent expression profiling of PTK2B and its relationship with Aβ, Tau and LRP-1 in hippocampus and blood of APPswe/PS1dE9

double-transgenic mouse. Zhongguo Ying Yong Sheng Li Xue Za Zhi 38:17–24. https://doi.org/10.10247/j.cjap.6191.2022.004
25. Harley P, Neves G, Riccio F, Machado CB, Cheesbrough A, R'Bibo L et al. (2022) Pathogenic TDP-43 disrupts axon initial segment structure and neuronal excitability in a human iPSC Model of ALS. bioRxiv
26. Harold D, Abraham R, Hollingworth P, Sims R, Gerrish A, Hamshere ML et al (2009) Genome-wide association study identifies variants at CLU and PICALM associated with Alzheimer's disease. Nat Genet 41:1088–1093. https://doi.org/10.1038/ng.440
27. Hong S, Prokopenko D, Dobricic V, Kilpert F, Bos I, Vos SJB et al (2020) Genome-wide association study of Alzheimer's disease CSF biomarkers in the EMIF-AD multimodal biomarker discovery dataset. Transl Psychiatry 10:403. https://doi.org/10.1038/s41398-020-01074-z
28. Hyman BT, Phelps CH, Beach TG, Bigio EH, Cairns NJ, Carrillo MC et al (2012) National Institute on Aging–Alzheimer's Association guidelines for the neuropathologic assessment of Alzheimer's disease. A&D 8:1–13. https://doi.org/10.1016/j.jalz.2011.10.007
29. Hyman BT, Trojanowski JQ (1997) Consensus recommendations for the postmortem diagnosis of Alzheimer disease from the National Institute on Aging and the Reagan Institute Working Group on diagnostic criteria for the neuropathological assessment of Alzheimer disease. J Neuropathol Exp Neurol 56:1095–1097. https://doi.org/10.1097/00005072-199710000-00002
30. Jacobson TY, Nho K, Risacher SL, Gao S, Shen L, Foroud T, et al. (2021) Genome wide analysis across Alzheimer's disease endophenotypes: main effects and stage specific interactions. medRxiv: 2021.2008.2013.21261887. https://doi.org/10.1101/2021.08.13.21261887
31. Jansen IE, Savage JE, Watanabe K, Bryois J, Williams DM, Steinberg S et al (2019) Genome-wide meta-analysis identifies new loci and functional pathways influencing Alzheimer's disease risk. Nat Genet 51:404–413. https://doi.org/10.1038/s41588-018-0311-9
32. Janson CG (2015) AD and CAA: Independent risk factors for dementia. Sci Trans Med 7:318ec214-318ec214. https://doi.org/10.1126/scitranslmed.aad9005
33. Jellinger KA (1998) The neuropathological diagnosis of Alzheimer disease. In: Jellinger K, Fazekas F, Windisch M (eds) Ageing and Dementia. Springer, Vienna City, pp 97–118
34. Josephs KA, Whitwell JL, Weigand SD, Murray ME, Tosakulwong N, Liesinger AM et al (2014) TDP-43 is a key player in the clinical features associated with Alzheimer's disease. Acta Neuropathol 127:811–824. https://doi.org/10.1007/s00401-014-1269-z
35. Kane JPM, Surendranathan A, Bentley A, Barker SAH, Taylor J-P, Thomas AJ et al (2018) Clinical prevalence of Lewy body dementia. Alzheimer's Res Ther 10:19. https://doi.org/10.1186/s13195-018-0350-6
36. Katsumata Y, Shade LM, Hohman TJ, Schneider JA, Bennett DA, Farfel JM et al (2022) Multiple gene variants linked to Alzheimer's-type clinical dementia via GWAS are also associated with non-Alzheimer's neuropathologic entities. Neurobiol Dis 174:105880. https://doi.org/10.1016/j.nbd.2022.105880
37. Koper MJ, Tomé SO, Gawor K, Belet A, Van Schoor E, Schaeverbeke J et al (2022) LATE-NC aggravates GVD-mediated necroptosis in Alzheimer's disease. Acta Neuropathol Commun 10:128. https://doi.org/10.1186/s40478-022-01432-6
38. Koper MJ, Van Schoor E, Ospitalieri S, Vandenberghe R, Vandenbulcke M, von Arnim CAF et al (2020) Necrosome complex detected in granulovacuolar degeneration is associated with neuronal loss in Alzheimer's disease. Acta Neuropathol 139:463–484. https://doi.org/10.1007/s00401-019-02103-y
39. Kunkle BW, Grenier-Boley B, Sims R, Bis JC, Damotte V, Naj AC et al (2019) Genetic meta-analysis of diagnosed Alzheimer's disease identifies new risk loci and implicates Aβ, tau, immunity and lipid processing. Nat Genet 51:414–430. https://doi.org/10.1038/s41588-019-0358-2
40. Lambert J-C, Heath S, Even G, Campion D, Sleegers K, Hiltunen M et al (2009) Genome-wide association study identifies variants at CLU and CR1 associated with Alzheimer's disease. Nat Genet 41:1094–1099. https://doi.org/10.1038/ng.439
41. Lee B, Yao X, Shen L, for the Alzheimer's Disease Neuroimaging I (2022) Genome-wide association study of quantitative biomarkers identifies a novel locus for Alzheimer's disease at 12p12.1. BMC Genom 23: 85. https://doi.org/10.1186/s12864-021-08269-8
42. Li C, Götz J (2018) Pyk2 is a novel tau tyrosine kinase that is regulated by the tyrosine kinase fyn. J Alzheimers Dis 64:205–221. https://doi.org/10.3233/jad-180054
43. McAleese KE, Walker L, Erskine D, Thomas AJ, McKeith IG, Attems J (2017) TDP-43 pathology in Alzheimer's disease, dementia with Lewy bodies and ageing. Brain Pathol 27:472–479. https://doi.org/10.1111/bpa.12424
44. Mirra SS, Heyman A, McKeel D, Sumi SM, Crain BJ, Brownlee LM et al (1991) The consortium to establish a registry for Alzheimer's disease (CERAD). Part II. Standardization of the neuropathologic assessment of Alzheimer's disease. J Neurol 41:479–486. https://doi.org/10.1212/wnl.41.4.479
45. Moore S, Evans LD, Andersson T, Portelius E, Smith J, Dias TB et al (2015) APP metabolism regulates tau proteostasis in human cerebral cortex neurons. Cell Rep 11:689–696. https://doi.org/10.1016/j.celrep.2015.03.068
46. Multhaup G, Huber O, Buée L, Galas M-C (2015) Amyloid Precursor protein (APP) metabolites APP intracellular fragment (AICD), Aβ42, and tau in nuclear roles*. JBC 290:23515–23522. https://doi.org/10.1074/jbc.R115.677211
47. Naj AC, Lin H, Vardarajan BN, White S, Lancour D, Ma Y et al (2019) Quality control and integration of genotypes from two calling pipelines for whole genome sequence data in the Alzheimer's disease sequencing project. Genomics 111:808–818. https://doi.org/10.1016/j.ygeno.2018.05.004
48. Nelson PT, Dickson DW, Trojanowski JQ, Jack CR, Boyle PA, Arfanakis K et al (2019) Limbic-predominant age-related TDP-43 encephalopathy (LATE): consensus working group report. Brain 142:1503–1527. https://doi.org/10.1093/brain/awz099
49. Nelson PT, Lee EB, Cykowski MD, Alafuzoff I, Arfanakis K, Attems J et al (2023) LATE-NC staging in routine neuropathologic diagnosis: an update. Acta Neuropathol 145:159–173. https://doi.org/10.1007/s00401-022-02524-2
50. Orme T, Guerreiro R, Bras J (2018) The genetics of dementia with lewy bodies: current understanding and future directions. Curr Neurol Neurosci Rep 18:67. https://doi.org/10.1007/s11910-018-0874-y
51. Park YH, Pyun JM, Hodges A, Jang JW, Bice PJ, Kim S et al (2021) Dysregulated expression levels of APH1B in peripheral blood are associated with brain atrophy and amyloid-β deposition in Alzheimer's disease. Alzheimers Res Ther 13:183. https://doi.org/10.1186/s13195-021-00919-z
52. Raux G, Gantier R, Thomas-Anterion C, Boulliat J, Verpillat P, Hannequin D et al (2000) Dementia with prominent frontotemporal features associated with L113P presenilin 1 mutation. J Neurol 55:1577–1578. https://doi.org/10.1212/wnl.55.10.1577
53. Rubinacci S, Ribeiro DM, Hofmeister RJ, Delaneau O (2021) Efficient phasing and imputation of low-coverage sequencing data using large reference panels. Nat Genet 53:120–126. https://doi.org/10.1038/s41588-020-00756-0
54. Serneels L, Van Biervliet J, Craessaerts K, Dejaegere T, Horré K, Van Houtvin T et al (2009) gamma-Secretase heterogeneity in the Aph1 subunit: relevance for Alzheimer's disease. Science 324:639–642. https://doi.org/10.1126/science.1171176
55. Soto-Faguás CM, Sanchez-Molina P, Saura CA (2021) Loss of presenilin function enhances tau phosphorylation and aggregation

in mice. Acta Neuropathol Commun 9:162. https://doi.org/10.1186/s40478-021-01259-7
56. Sperling RA, Aisen PS, Beckett LA, Bennett DA, Craft S, Fagan AM et al (2011) Toward defining the preclinical stages of Alzheimer's disease: recommendations from the National Institute on Aging-Alzheimer's Association workgroups on diagnostic guidelines for Alzheimer's disease. Alzheimers Dement 7:280–292. https://doi.org/10.1016/j.jalz.2011.03.003
57. Spillantini MG, Schmidt ML, Lee VMY, Trojanowski JQ, Jakes R, Goedert M (1997) α-Synuclein in Lewy bodies. Nature 388:839–840. https://doi.org/10.1038/42166
58. Talyansky S, Le Guen Y, Kasireddy N, Belloy ME, Greicius MD (2023) APOE-ε4 and BIN1 increase risk of Alzheimer's disease pathology but not specifically of Lewy body pathology. Acta Neuropathol Commun 11:149. https://doi.org/10.1186/s40478-023-01626-6
59. Tampi RR, Forester BP, Agronin M (2021) Aducanumab: evidence from clinical trial data and controversies. Drugs Context. https://doi.org/10.7573/dic.2021-7-3
60. Tan M-S, Yang Y-X, Xu W, Wang H-F, Tan L, Zuo C-T et al (2021) Associations of Alzheimer's disease risk variants with gene expression, amyloidosis, tauopathy, and neurodegeneration. Alzheimer's Res Ther 13:15. https://doi.org/10.1186/s13195-020-00755-7
61. Thal DR, Ghebremedhin E, Rüb U, Yamaguchi H, Del Tredici K, Braak H (2002) Two types of sporadic cerebral amyloid angiopathy. J Neuropathol Exp Neurol 61:282–293. https://doi.org/10.1093/jnen/61.3.282
62. Thal DR, Rüb U, Schultz C, Sassin I, Ghebremedhin E, Del Tredici K (2000) Sequence of Aβ-protein deposition in the human medial temporal lobe. J Neuropathol Exp Neurol 59:733–748. https://doi.org/10.1093/jnen/59.8.733
63. van Dyck CH, Swanson CJ, Aisen P, Bateman RJ, Chen C, Gee M et al (2023) Lecanemab in early Alzheimer's disease. N Engl J Med 388:9–21. https://doi.org/10.1056/NEJMoa2212948
64. Vonsattel JP, Myers RH, Hedley-Whyte ET, Ropper AH, Bird ED, Richardson EP Jr (1991) Cerebral amyloid angiopathy without and with cerebral hemorrhages: a comparative histological study. Ann Neurol 30:637–649. https://doi.org/10.1002/ana.410300503
65. Voyle N, Keohane A, Newhouse S, Lunnon K, Johnston C, Soininen H et al (2016) A pathway based classification method for analyzing gene expression for Alzheimer's disease diagnosis. J Alzheimers Dis 49:659–669. https://doi.org/10.3233/jad-150440
66. Wiersma VI, van Ziel AM, Vazquez-Sanchez S, Nölle A, Berenjeno-Correa E, Bonaterra-Pastra A et al (2019) Granulovacuolar degeneration bodies are neuron-selective lysosomal structures induced by intracellular tau pathology. Acta Neuropathol 138:943–970. https://doi.org/10.1007/s00401-019-02046-4
67. Wightman DP, Jansen IE, Savage JE, Shadrin AA, Bahrami S, Holland D et al (2021) A genome-wide association study with 1,126,563 individuals identifies new risk loci for Alzheimer's disease. Nat Genet 53:1276–1282. https://doi.org/10.1038/s41588-021-00921-z
68. Wisniewski T, Drummond E (2020) APOE-amyloid interaction: therapeutic targets. Neurobiol Dis 138:104784. https://doi.org/10.1016/j.nbd.2020.104784
69. Wu M, Fang K, Wang W, Lin W, Guo L, Wang J (2019) Identification of key genes and pathways for Alzheimer's disease via combined analysis of genome-wide expression profiling in the hippocampus. Biophys Rep 5:98–109. https://doi.org/10.1007/s41048-019-0086-2
70. Zhang X, Zhang C, Prokopenko D, Liang Y, Han W, Tanzi RE et al (2020) Negative evidence for a role of APH1B T27I variant in Alzheimer's disease. Hum Mol Genet 29:955–966. https://doi.org/10.1093/hmg/ddaa017
71. Zhu J, Liu X, Yin H, Gao Y, Yu H (2021) Convergent lines of evidence support BIN1 as a risk gene of Alzheimer's disease. Hum Genom 15:9. https://doi.org/10.1186/s40246-021-00307-6